Indirect Current Control Algorithm Implementation and Validation, for Active Filtering Using Constant Switching Frequency Hysteresis Controllers

Mihaita LINCA, Constantin Vlad SURU, Cristina Alexandra PREDA

University of Craiova/Department of Electromechanical, Environmental and Industrial Informatics,
Craiova, Romania, mlinca@em.ucv.ro, vsuru@em.ucv.ro, apreda@em.ucv.ro

Abstract - **The aim of this paper is the implementation and the experimental validation of a constant switching frequency hysteresis current controller as a part of an active filtering system control algorithm, based on the indirect current control. The classical choices in the literature are the hysteresis current controller and the PI controller both with their corresponding advantages and disadvantages. A solution which achieves the advantages of both classical hysteresis and PI controllers is the constant switching frequency hysteresis current controller. This controller can be obtained by combining the hysteresis comparators with the PWM suboptimal modulator. The performances of the active filtering system based on the indirect current control and the proposed controller are compared with the corresponding performances obtained by the same system implemented with the well documented PI current controller. The regulator implementation and performance comparative study were accomplished on a comprehensive experimental active filtering system based on the dSpace DS1103 prototyping board.**

Cuvinte cheie: filtru activ, controlul curentului, regulator cu histerezis,regulator PI.

Keywords: *active compensator, current control, hysteresis controller, PI controller.*

I. INTRODUCTION

The shunt active power filters typically use two control loops, for the regulation of the compensating capacitor voltage, and for the controlled current at the point of common coupling (which is the filter output current for the direct current control, and the current absorbed from the power grid by the filtering system, for the indirect current control [1-6]).

The capacitor voltage controller is a PI controller and the three current controllers can be one of two types [1-6]:

- PI controllers, one for each phase, the PWM modulator giving the constant switching frequency, with superior performances obtained at the cost of elaborate parameter tuning, but dependent on the system structure and constants;

- hysteresis controllers, one for each phase, which are simple and robust, the parameter tuning also being avoided, but the constant hysteresis band giving variable switching frequency.

The constant switching frequency hysteresis current controllers combine the hysteresis comparators with the suboptimal modulator of the PI control loop. The modulator carrier frequency imposes the switching frequency which is the constant frequency of the hysteresis band [8].

The first section of the paper is the introduction, and in the second chapter the shunt active compensator control algorithm is described, for the adopted solution of indirect current control. The constant switching frequency hysteresis current controller is substantiated in the third chapter. Its implementation and simulation results are described in the fourth chapter. Finally, the experimental setup is described in the fifth chapter, the experimental obtained results in the sixth chapter, and finally and the conclusions are drawn.

II. THE ACTIVE COMPENSATOR CONTROL ALGORITHM

The shunt compensator control algorithm is depicted in Fig. 1. For the indirect current control, the dc-link voltage control loop gives the amplitude of the current flowing from the power grid to the active compensating system, in order to charge the compensating capacitor [4-6]. To obtain the prescribed currents, the voltage regulator output is multiplied with a three phase system of unitary amplitude signals, in phase with the grid voltage (the voltage template). To obtain these signals, a phase locked loop is necessary [5].

The current loop controls the current absorbed from the power grid by the entire filtering system. The current loop is typically implemented with a hysteresis controller (per phase) or less often with a PI controller (followed by a PWM modulator) [3], or a constant switching frequency hysteresis controller [8]. The output of the current loop is the gating signals vector, despite the current controller type.
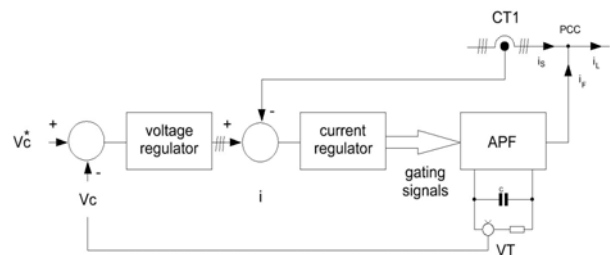

Fig. 1. The active compensator indirect current control algorithm.

There are multiple ways to obtain the constant switching frequency for the hysteresis regulator, by continuously adapting the hysteresis band, dependently on the controlled current rate of rise [7], by over modulating the current error [8-9], or by using a fuzzy current regulator [10]

III. THE HYSTERESIS CURRENT CONTROLLER WITH CONSTANT SWITCHING FREQUENCY

The hysteresis regulator generates the gating signals for each inverter leg based on the current error on the corresponding phase (Fig. 2). The current error slides between the hysteresis band maximum or minimum limit, when the output changes its state. This gives a constant band with variable switching frequency [9].

For the hysteresis controller, on the indirect current control, the switching frequency value is given by the sum of the falling and rising intervals of the grid current, for each switching period [9]:

$$f_{sw} = \frac{1}{t_1 + t_2} \qquad (1)$$

$$t_1 = \frac{hys}{u_{max} - u_{eq}} \qquad (2)$$

$$t_2 = \frac{hys}{u_{eq} - u_{min}} \qquad (3)$$

The quantities u_{max}, u_{min}, and u_{eq} are the upper limit, the lower limit and the equivalent output values. The latter is the average value of the active compensator output (i.e. the voltage applied between the power grid and the inverter output) and is defined as [9]:

$$u_{eq} = \frac{R}{L} \cdot i_F + \frac{di_F}{dt} \qquad (4)$$

In (4) R and L are the resistance and inductance of the 1st order interface filter, and i_F is the active filter output current. For the indirect current control, the filter output current, i_F, is obtained intrinsically by maintaining the compensating capacitor voltage. Although, the current loop controls the grid current, the filter equivalent output, u_{eq}, varies between the rated limits, so the filter current also varies between its rated limits. Concluding, the current absorbed by the nonlinear loads must be kept under the rated value, to not exceed the stated limits.

The switching frequency is therefore variable and influenced several elements, such as: the hysteresis band, the active filter output current rate of rise, the interface filter inductance, and its voltage drop, which is very important. The maximum value of the switching frequency is reached when u_{eq} is null, and is given by [9]:

$$f_{sw\,max} = \frac{1}{4hys} \cdot (u_{max} - u_{min}) \qquad (5)$$

In an equivalent manner, the lowest switching frequency value is null and is reached when the equivalent output of the active compensator, u_{eq}, is equal to u_{max} or $u_{min.}$
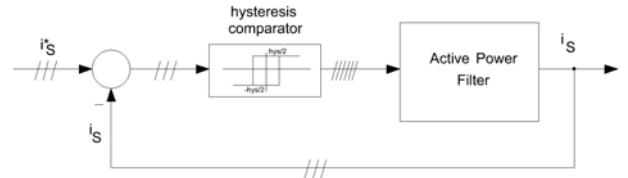

Fig. 2. The current control diagram using the hysteresis controller

The constant switching frequency current controller is obtained from the classical hysteresis type by over-modulating the current error with an triangular carrier signal, i_r before being applied to the comparators (Fig. 3) [9].

The switching frequency is now constant, given by the carrier signal, i_r, frequency. The rising time, t_1, and the falling time, t_2 are [9]:

$$T_{sw} = t_1 + t_2 \qquad (6)$$

$$(u_{eq} - u_{min}) \cdot t_1 = (u_{max} - u_{eq}) \cdot t_2 \qquad (7)$$

Therefore, the current ripple is variable, depending on the equivalent output of the current controller (the dc-link voltage, power grid voltage and the interface filter inductance are constant) [9]:

$$\Delta i = \frac{(u_{max} - u_{eq}) \cdot (u_{eq} - u_{min})}{u_{max} - u_{min}} \cdot \frac{T_{sw}}{2} \qquad (8)$$

The current error average value applied to the PWM modulator, varies in normal operation between the carrier positive amplitude and negative amplitude, and must not exceed these limits [9]:

$$err_{avg} = \frac{2u_{eq} - (u_{max} + u_{min})}{u_{max} - u_{min}} \cdot i_{r\,max} \qquad (9)$$

From (9) it results that when u_{eq} varies between u_{min} and u_{max}, then the average current error varies between the the carrier positive amplitude and negative amplitude.

Therefore, when the filter current has a high rate of rise, the current error could overrun the triangular carrier amplitude, and consequently, the active filter output will tend to exceed its limits, the filter being unable to obtain the prescribed current.

To ensure proper operation, it is mandatory that the carrier rate of rise is high enough, compared to current error's rate of rise.
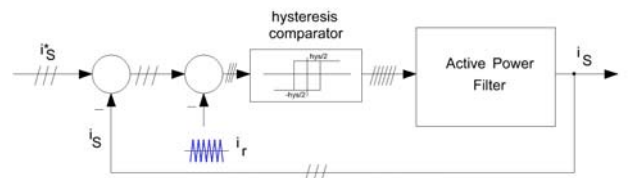

Fig. 3. The current control diagram using the constant switching frequency hysteresis controller

IV. VIRTUAL IMPLEMENTATION OF THE ACTIVE FILTERING SYSTEM

The virtual implementation of the active filtering system is a Simulink model which contains all the system components built with SimPowerSystems or Simulink library blocks, as necessary (Fig. 5). The system components with their corresponding rated powers are the following:

- Active compensator:
  - U_N = 380V, I_N = 25 A;
  - Dc-link capacitor: 1100 μF;
  - Interface inductor: 4.4 mH;

- Nonlinear Load (three phase diode rectifier with resistive load):
  - U_N = 380V, I_N = 15A;
  - S_N = 9.84 kVA; P_N = 9.4 kW; Q_N = 0 kvar.

- The active filter control block (which contains the power grid current and capacitor voltage regulating loops [2], auxiliary blocks for the active filter start-up process [11] control and signal processing blocks, respectively);
- Auxiliary measurement and computation blocks.

The virtual system replicates the experimental system regarding both its structure and rated parameters. Although the load power factor is 0.95, so not very low, the active filter is put to the test because of the load current high current rise and high THD.

In order to rate the performances of the constant switching frequency hysteresis controller, the obtained results were compared to the PI regulators corresponding results. So, the current loop in the control algorithm section of the model in Fig. 4 had two variants:

- The implementation based on the constant switching frequency hysteresis regulator (Fig. 5-b), (obtained by modifying the classical hysteresis regulator - Fig. 5-a and c);
- The implementation of the PI regulator (Fig. 5-c).

It can be seen that both loops uses the PWM suboptimal modulator which imposes the switching frequency on one hand, and requires low sample time on the other hand. Therefore, the overall performances of both regulators are influenced in the same way by the simulation time step, which is critical for the carrier shape generation.

The PI regulator parameters were determined for the above rated values of the active filtering system based on the optimum modulus criterion [2]:

- K_p = 2.5;
- T_i = 3.19 · 10^{-5}.

The both studied regulators are using a validation signal (*en*) with two purposes:

- the gating signals are applied to the power inverter only when the control loops are validated by the start-up control block [11] (when the dc-link capacitor is charged at about 90% of the power grid voltage amplitude);
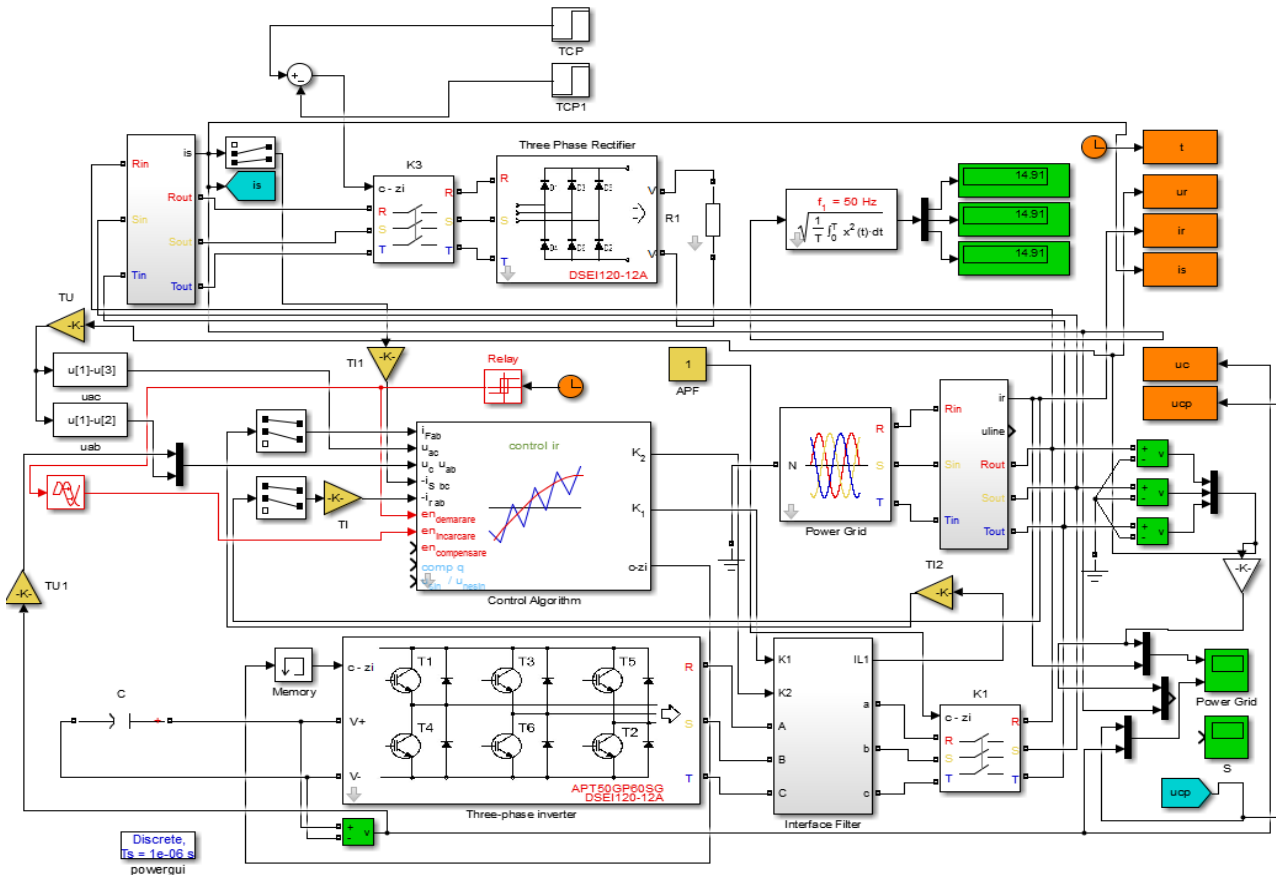- the PI regulators are kept inactive as long as en = 0.

Fig. 4. The active filtering system complete model
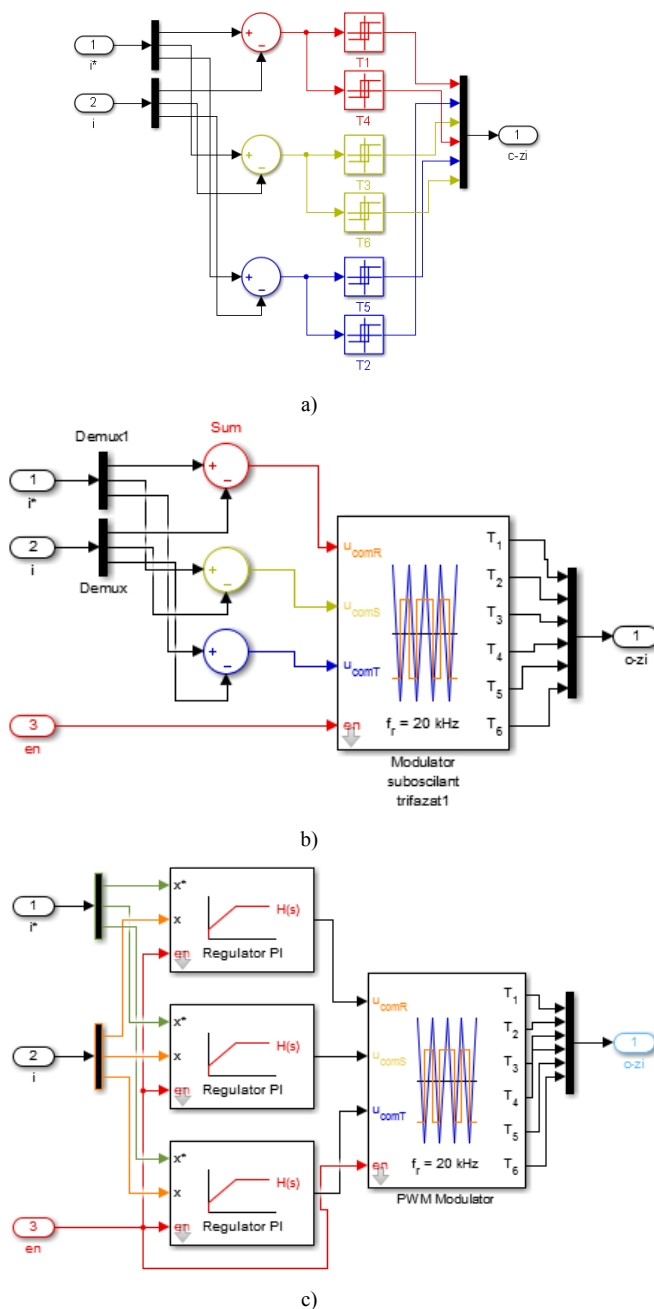
a)

b)

c)

Fig. 5. The current control loop: a) the initial hysteresis controller, b) the hysteresis controller with constant switching frequency, c) based on the PI regulator

The active filtering system in Fig. 4 was studied by simulation for the two current regulator types.

The steady state current absorbed by the distorting load and its harmonic spectra are presented in Fig. 6. The RMS value of the load current on each phase is 15 A. The total harmonic distortion factor is 30.68%, for sinusoidal grid voltage.

The first case study corresponds to the hysteresis controller with constant switching frequency. In this case, the waveform corresponding to the current flowing from the power grid to the filtering system is presented in Fig. 7-a. The harmonic spectra of this current are presented in Fig. 7-b, respectively.

The grid current total harmonic distortion factor is 13.44%, giving a filtering efficiency of just 2.28. The

partial harmonic distortion factor is 11.65%, showing that most of the current distortion is below the 51th harmonic. This can be proved by the current waveform which is sinusoidal (not considering the current ripple - Fig. 7-a) but with visible current spikes, generated by the active filter incapacity to compensate the load current steep rises. Therefore, the harmonic spectra highlights the presence of odd harmonics improper compensated (5th, 7th, 11th,13th, etc - Fig. 7-b). At the same time, the current ripple is not constant, a specific issue of the PI current regulator, showing the constant switching frequency.

Regarding the power factor compensation, the power factor before compensation is 0.9560 and after compensation is 0.9912. Another important fact is the power consumed by the active filter from the power grid which is 0.891 kW. It must be mentioned that the switching frequency is 20 kHz (at a simulation time step of 1 μs.

The obtained results were compared with the "reference" results obtained with an active filtering system well documented in the literature (Fig. 5-c) [1-3].

The current absorbed from the power grid by the "reference" active filtering system and its harmonic spectra are presented in Fig. 8. The grid current total harmonic distortion factor in this case is 15.11%, a close yet lower value to the one obtained with the investigated system, resulting in a filtering efficiency of 2.03. The partial harmonic distortion factor on the other hand, is 13.32%, showing again a worse result obtained by the PI regulators.
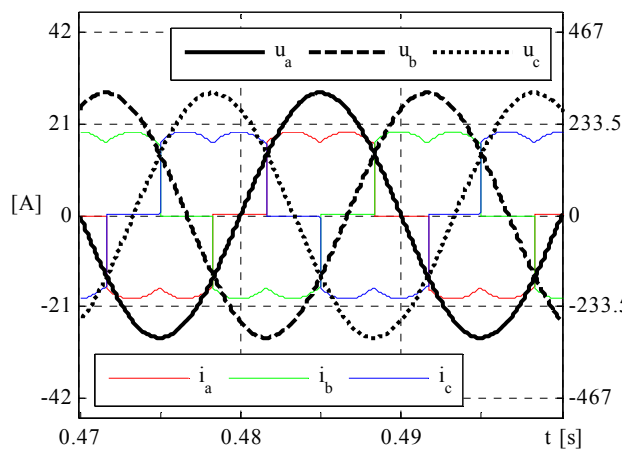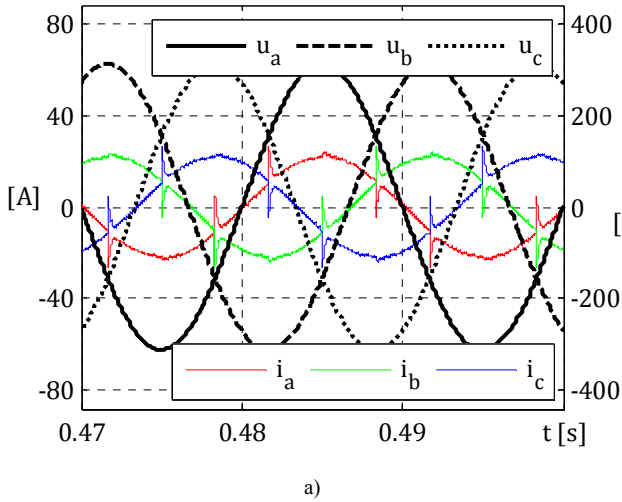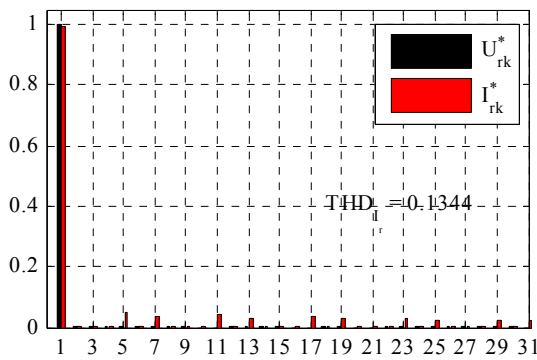

a)
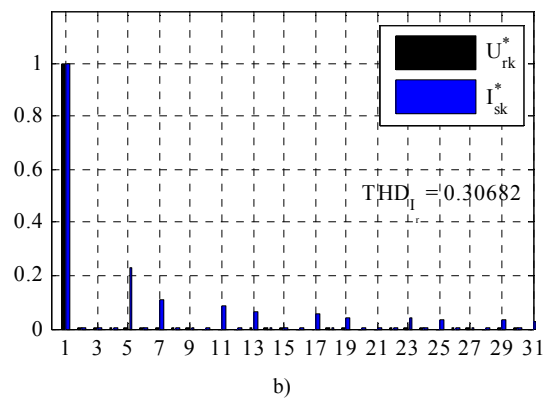
b)

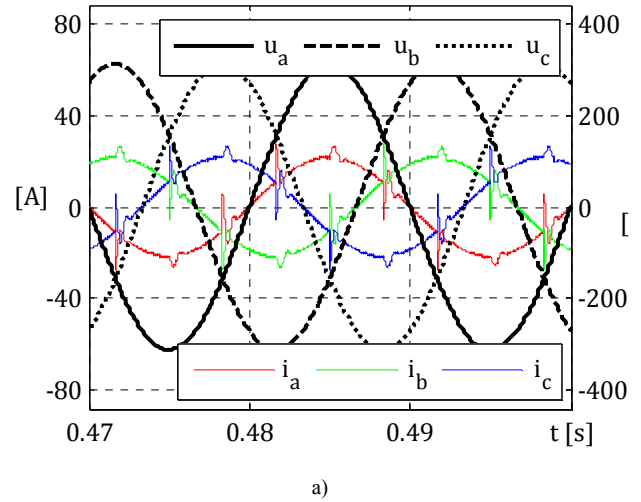Fig. 6. The current absorbed by the nonlinear load (a) and its harmonic spectra

Fig. 7. The current flowing from the power grid to the active compensation system (a) and its harmonic spectra, for the hysteresis controller with constant switching frequency

Fig. 8. The current flowing from the power grid to the "reference" active compensation system (a) and its harmonic spectra, for the PI current controller

Also, the worse result obtained by the PI control loop can be visually observed from the compensated current waveform, in which the regulators tend to oscillate at the rectifier switching times.
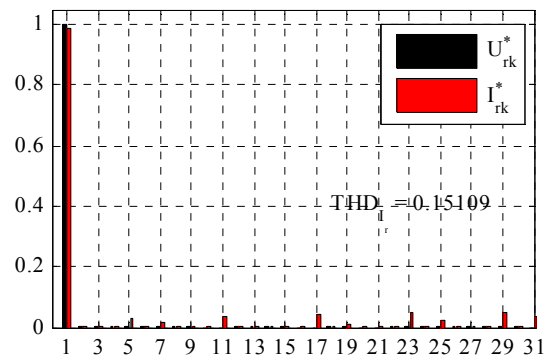
It must be mentioned that the compensating capacitor voltage control loop is identical for the two studied cases, so the distortion introduced by the voltage regulator output ripple is as high as 1.78%.

Regarding the power factor, in this case, after compensation we have 0.9896, slightly lower. The power consumed by the active filter from the power grid, for the PI current regulation is 0.820 kW, 50 W lower.

Because the output of the voltage regulator (which is the amplitude of the desired grid current) is not constant, even in steady state operation, the compensated desired current is distorted from the start, but this distortion is equally imposed to the both current regulators. So, in order to eliminate the influence of the voltage regulator (output ripple), the compensating current was investigated for the both regulator types, compared to prescribed compensating current. Because for the indirect current principle the compensating current computation is not necessary (this current results intrinsically to maintain a sinusoidal current from the power grid, the polluting load current being a disturbance) the necessary compensating current was estimated from the power grid desired current (sinusoidal active current) and the load current.

The compensating current is illustrated in Fig. 9-a for the constant switching frequency hysteresis controller and in Fig. 9-c for the PI controller. It can be seen that for the both controllers a visible deviation exists, in about the same places on the current waveform (excepting the current oscillation of the PI control). This means that a similar fault is encountered for both controllers; therefore the common element is responsible. The faulty element is the PWM modulator - because of the simulation time step, the triangular carrier is not well synthetized. More specifically, the carrier amplitude is bent, because of the insufficient number of sampling points (for the 1μs simulation time step and 20 kHz triangular carrier frequency).

The effect of this fault is that the current error (in the case of the hysteresis regulator) and the controller output (in the case of PI regulator) exceeds the carrier amplitude which is lower than 10).

This can be seen in the switching frequency (Fig. 9-b and d), which is not constant at the imposed value of the carrier (20 kHz) but drops several times. The time moments where the switching frequency varies are the exact moments when the PWM modulator input exceeds the bended carrier amplitude, the current loop no longer controlling the active filtering system. This effect is more pronounced for the PI regulator, affecting the compensation performance (the performance is also affected by the current overshoot – Fig. 9.d).
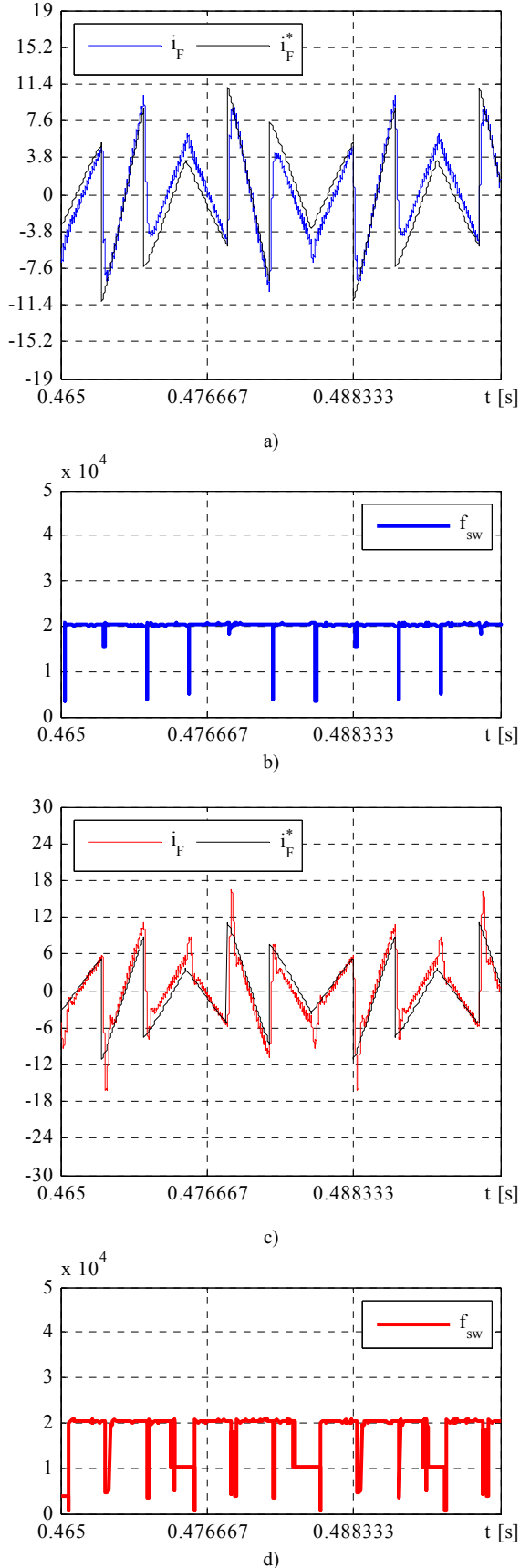
a)

b)

c)

d)

Fig. 9. The compensating current (a) and switching frequency (b) for
the hysteresis controller with constant switching frequency, and
for the PI controller (corresponding c and d)

V. THE EXPERIMENTAL SETUP AND RESULTS

The experimental active filtering system structure is the same as for the virtual system, with the same rated values as stated in the previous section. The virtual system was built to replicate the experimental system in order to have relevant and comparable results. The control section of the active filter was implemented based on a dSpace DS1103 prototyping board. So the control algorithm of the active filter was the same Simulink block as for the virtual system, but with the SimPowerSystems block replaced with the corresponding DS1103 real time interface blocks (Fig. 10) [13-15].

The PWM suboptimal modulator used for the both control loops was the hardware PWM modulator of the DS1103. This way, the triangular carrier was not influenced by the control board time step (being a hardware system the time step is significantly higher in this case, 20 μs as for 1 μs in simulation). For this time step the carrier would be impossible to generate for the frequency of 20 kHz.

The PI regulator parameters were the same as in the virtual study, as the system parameters are the same.

The active filter real time control and monitoring was done by means of the virtual control panel built in the dSpace board specific software, illustrated in Fig. 11. The virtual instruments of the control panel are connected with the control algorithm (Fig. 10) Simulink variables and signals. This way the system was controlled and monitored as follows [13-15]:

- The validation of the control loops, therefore the active filter start-up (compensating capacitor charging and intrinsic compensation) was done by Simulink signals generated by means of *Constant* blocks and their corresponding variables (Fig. 10);
- The important variable signals (like power grid voltages and currents) were real time plotted on virtual oscilloscopes (*Time Plotter*) connected with Simulink signals (from ADC-s or computed model signals);
- Quantities like mean and RMS values were computed in the Simulink model by the corresponding blocks and displayed on the control panel using virtual meters (Fig. 11).
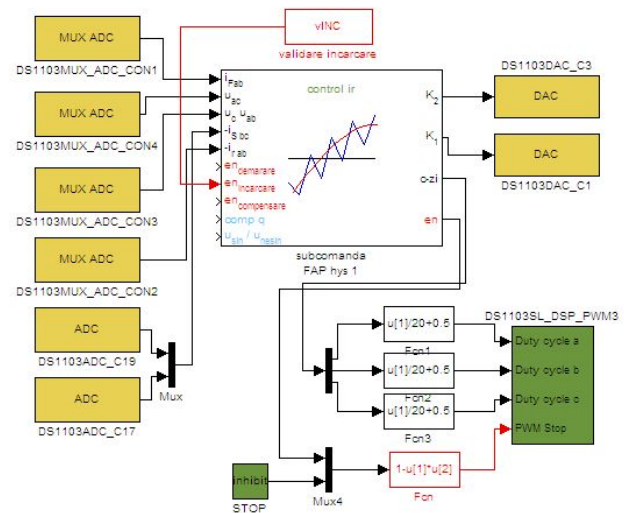

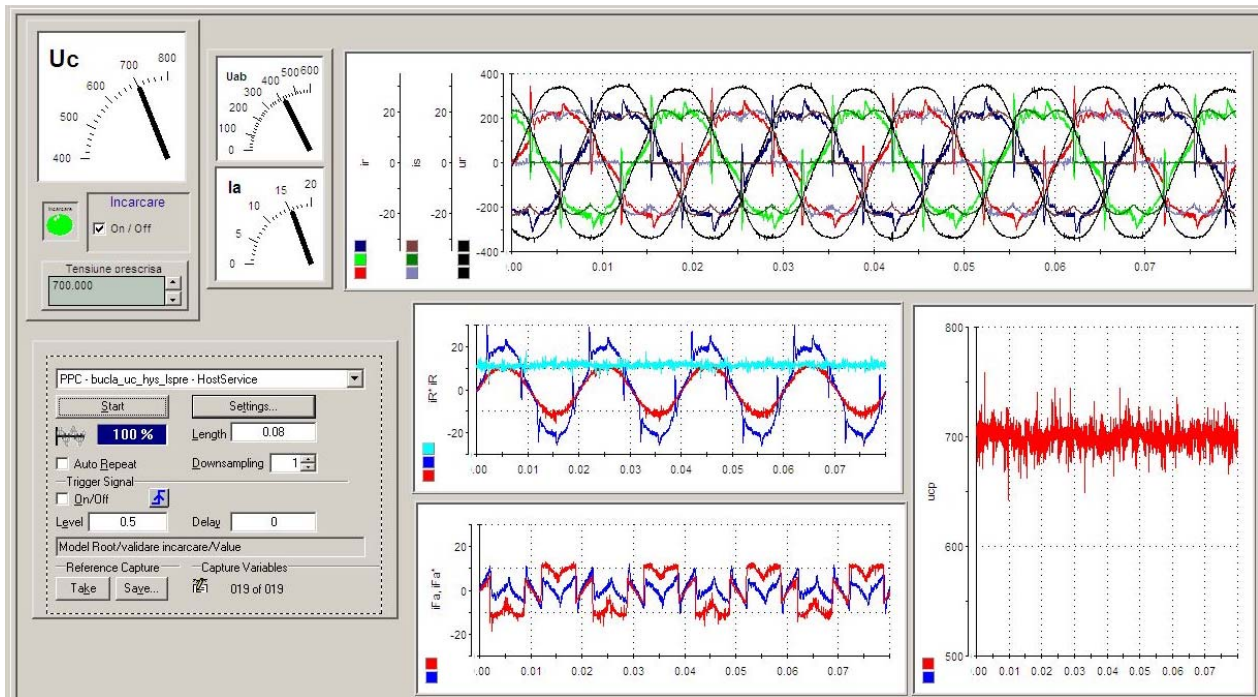Fig. 10.   The experimental active filter control algorithm

Fig. 11.   The experimental active filter virtual control panel

The investigated signals were sampled using both DS1103 analog to digital converters and the Tektronics MSO 4104B-L digital oscilloscope. This way the sampled signals were used for numerical analysis - the advantage of using the dSpace board ADC-s to acquire the data for the digital analysis (instead of the digital oscilloscope) is that it saves the sample data directly as a Matlab *.mat file (and the migration of the sampled data from the digital oscilloscope memory to Matlab is no longer necessary).

The grid voltage and current (on one phase) sampled with the Tektronix oscilloscope are illustrated in Fig. 12-a; the same signals sampled with the DS1103 board ADC-s and the computed harmonic spectra are illustrated in Fig. 12, b and c.

The power grid voltage THD at the experiment time is 2.72% and the polluting load current THD is 29.94%, for a RMS value of 15.11 A. The active power consumed by the load is 10.73 kW at a power factor of 0.9621.

For the first investigated case, the constant switching frequency hysteresis controller, the power grid voltage and current are illustrated in Fig. 13.

It can be seen that the compensated (grid) current is almost sinusoidal, but with visible deviations. From the wave form it results that the current has two distinct distortions:

-   Caused by the active filter incapacity to compensate the steep transitions of the load current during diode switching;
-   Caused by the control algorithm, precisely by the high time step imposed by the dSpace DS1103 control board (20 µs).

Although the PWM modulator is implemented hardware so the dSpace time step it should not influence the carrier synthetizing, the compensated current waveform is still affected. It worth mentioning that the switching frequency had to be reduced from 20 kHz to 8 kHz, in order to obtain minimum results. This is because considering the working principle of the constant switching frequency hysteresis controller [8-9] the carrier rate of rise must be comfortably higher than the current error higher rate of rise. For the switching frequency of 20 kHz and the time step of 20 µs this condition is not satisfied. When this happens the compensating current cannot follow the imposed current as the PWM modulator becomes saturated. As more as the switching frequency is reduced (the time step is already the lowest), the more the stated condition is satisfied.

The distortion can be seen also on the harmonic spectra in which the slight compensation of 5th and 7th harmonics is followed by the amplification and generation of other low order harmonics.

Numerically, the compensated current THD is 20.86% giving a filtering efficiency of 1.43. The partial harmonic distortion factor for this case is 20.17 showing that almost all harmonic content is below 51th harmonic.

The compensated power factor is 0.9783 (from 0.9621) with a consumed power (of the active filter) of 220 W.

In the case of the reference system (the PI control implementation) the power grid voltage and current are illustrated in Fig. 14.

It can be seen that the compensated (grid) current is again almost sinusoidal, but with visible deviations:

-   Caused by the active filter incapacity to compensate the steep transitions of the load current during diode switching (the load and the APF interface filter are the same);
-   Caused by the control algorithm, as the current control loop tends to oscillate (this is the most pronounced as the nonlinear load current rate of rise is higher - for example, at the rectifier diode switching times).
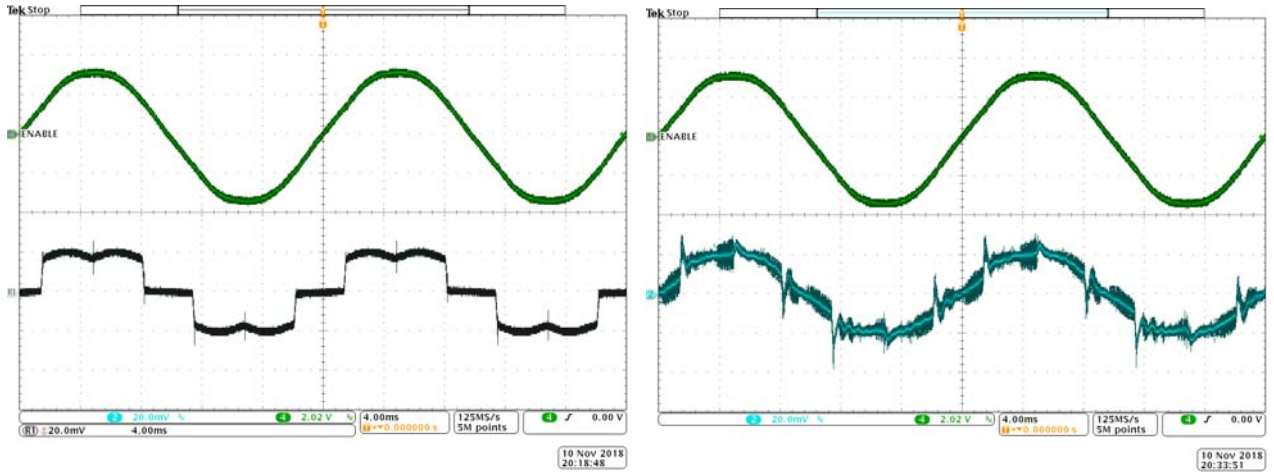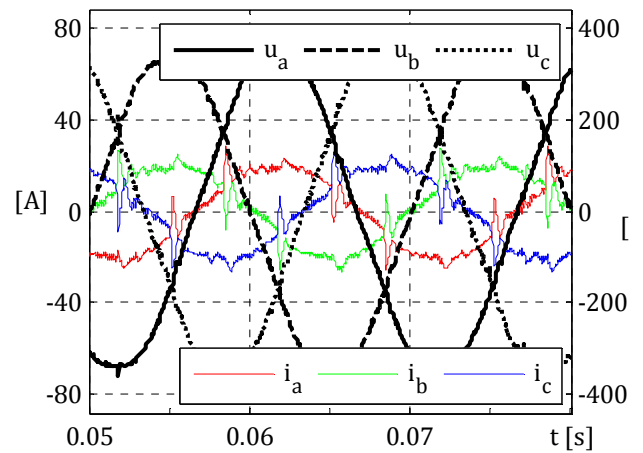
a)
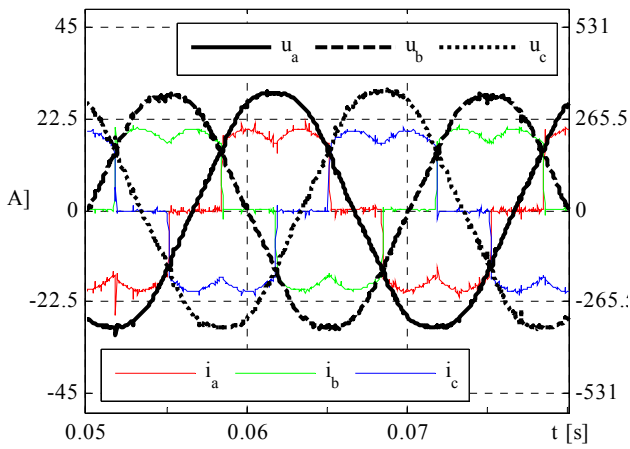
b)
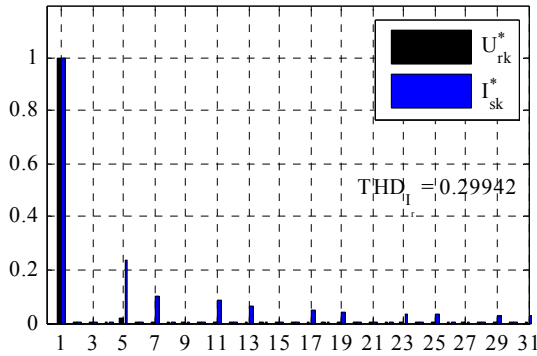
c)

Fig. 12. The current absorbed by the nonlinear load sampled with the Tektronics MSO 4104B-L (a), the DS1103 ADC-s (b) and its harmonic spectra (c)
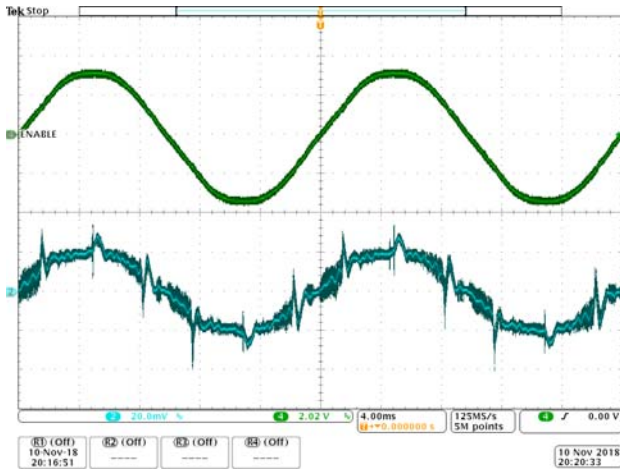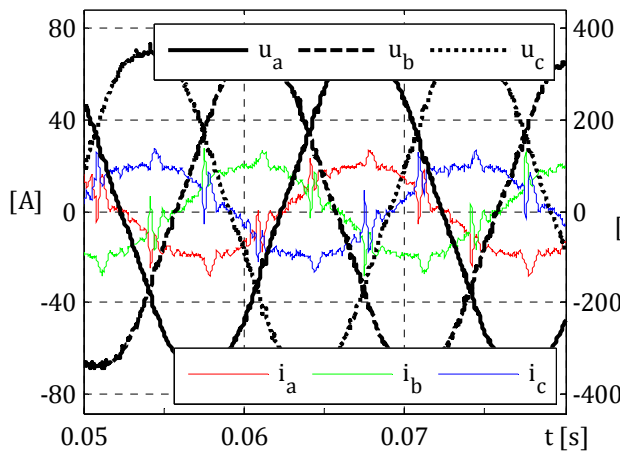

c)

Fig. 13. The compensated current for the constant switching frequency hysteresis controller: a) sampled with the Tektronics MSO 4104B-L, b) sampled with the DS1103 ADC-s, c) harmonic spectra

An interesting fact about the switching frequency is that if for the case of the constant switching frequency hysteresis regulator the performance decreases with the increase of the switching frequency, for the PI controller the situation is opposite.

Now, as more the switching frequency decreases from the starting value of 20 kHz, the more the system tends to oscillate. This trend was observed also in the simulation and is caused by the PI controllers.

Numerically, the compensated current THD is 18.84% giving a filtering efficiency of 1.57, a slightly better result compared to the investigated controller. The partial harmonic distortion factor is 18.29%, showing on one hand that almost all harmonic content is below 51th harmonic, and on the other hand that the switching distortion is very low for the 20 kHz frequency..
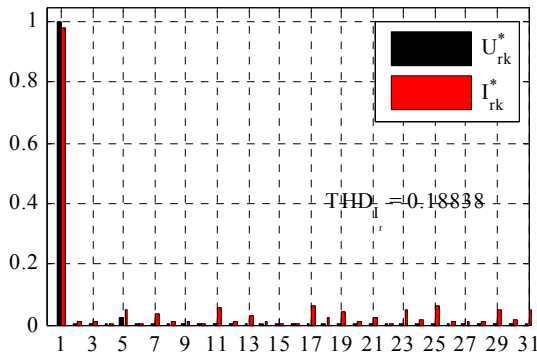
The compensated power factor is better, 0.9813 (from 0.9631), with the same consumed power (of the active filter) of 220 W.
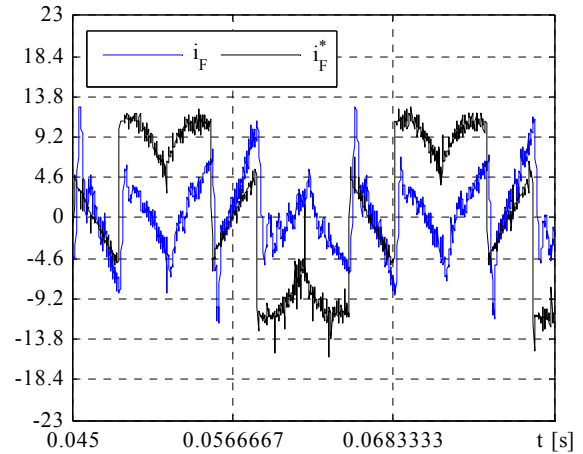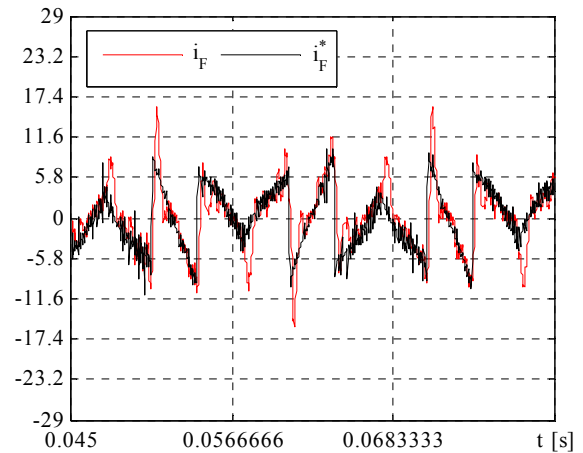
Fig. 14. The compensated current for the PI control: a) sampled with the Tektronics MSO 4104B-L, b) sampled with the DS1103 ADC-s, c) harmonic spectra

To investigate the cause of the compensated current distortion, the resulted compensating current was plotted, for the two investigated cases, based on the sampled data (Fig. 15):

- The active filter output current (compensating current sampled by the DS1103 ADCs;
- The imposed compensating current (Simulink signal, recorded by the DS1103), estimated from the power grid desired current (sinusoidal active current) and the load current (sampled by the DS1103 ADCs).

Fig. 15. The compensating current for: a) the constant switching frequency hysteresis controller, b) PI controller

The compensating current illustrated in Fig. 15 for the both controllers shows that in the case of PI control the difference between the imposed current and the real current consists on the problems highlighted by the compensated current (the poor compensation of the steep rises of the load current due to the limitations of the active filter interface filter on one hand and the controller oscillations on the other hand).

Regarding the constant switching hysteresis controller, the problem is a lot more different, showing that the imposed compensating current differs visibly from the real current. Considering the fact that the compensated current shape is almost correct, it results that the imposed current is wrong. This can also be seen in Fig 11, when the active filter virtual control panel displays the same currents plotted in Fig. 15-a, but also the grid currents. In this particular oscilloscope the real grid current (blue) is displayed with the imposed grid current (red) and the compensating capacitor voltage regulator output (cyan). It can be seen that the imposed current amplitude (voltage controller output) is lower that it should be: about 11A, when the nonlinear load active current RMS value is about 15A giving amplitude of about 21A.

As stated before, this system response is due to the relatively high time step (20 μs) in combination with a rela-

tively low switching frequency. This makes the carrier rate of rise to be not as high as necessary compared to the current error rate of rise. The limitation is that the current error rate of rise is limited and affected by the time step which cannot be lower than 20 μs. This way, the hardware carrier can be as high as 20 kHz or even higher, but the system is nonresponsive for large period of times (compared to the carrier period) making the system to respond incorrectly.

CONCLUSIONS

The comparative study of performances obtained by the hysteresis controller with constant switching frequency proves the validity of this concept and also, its correct implementation. The simulation results showed very good results of the investigated controller compared to the PI controller, for a sufficiently low simulation step. The performances are, of course, dependent on the active filter power section limitations – because of the simple first order interface filter, the diode switching steep current rises are impossible to be compensated by both controllers.

In the experimental implementation, though, the performances drops as the computing hardware limitations keep the time step too high. This conclusion can be drawn for both controllers, the relatively high time step having a negative influence on the system response. In the case of the constant switching hysteresis controller the system responds incorrectly, being the more ineffective as the ratio between the carrier period and the time step lowers. Although, the "reference" system (PI control) is also affected, the PI controller's response being dependent on the time step. However, the PI control system was the more unstable the ratio between the carrier period and the time step increases.

The constant switching frequency hysteresis controller operates with similar performances as the PI current controller, giving excellent performance, but with at least the same constraints related to the required computing power as the PI control.

REFERENCES

[1] Popescu Mihaela, Bitoleanu A, Suru V., A DSP-Based Implementation of the p-q Theory in Active Power Filtering Under Nonideal Voltage Conditions, IEEE Transactions on Industrial Informatics, Volume 9 , Issue 2, ISSN 1551-3203, May 2013, pp. 880-889.

[2] Popescu Mh., Bitoleanu A., Dobriceanu M., Suru V., "Optimum Control Strategy of Three-Phase Shunt Active Filter System", Proceedings of World Academy of Science, Engineering and Technology, Vol. 58, October 2009, ISSN 2070-3724, pp.245-250.

[3] Constantin Vlad Suru, Mihaita Linca, Cristina Alexandra Patrascu, Evaluation of current control methods in three-phase shunt active power filters system, Analele Universitatii Eftimie Murgu Resita Fascicola de Inginerie, ANUL XXI, NR. 3, 2014, ISSN 1453 - 7397, pp 177-188.

[4] Bitoleanu A, Popescu M, Suru CV, Theoretical and Experimental Evaluation of the Indirect Current Control in Active Filtering and Regeneration Systems, Published in: International Conference on Optimization of Electrical and Electronic Equipment (OPTIM) & 2017 Intl Aegean Conference on Electrical Machines and Power Electronics (ACEMP), 2017, 25-27 May 2017, Electronic ISBN: 978-1-5090-4489-4 USB ISBN: 978-1-5090-4488-7, Page(s): 759-764.

[5] Bitoleanu, Alexandru; Popescu, Mihaela; Suru, Vlad, Optimal Controllers Design in Indirect Current Control System of Active DC-Traction Substation, Conference: 17th IEEE International Power Electronics and Motion Control Conference (PEMC), IPEMC Pages: 912-917, Published: 2016, ISBN:978-1-5090-1798-0.

[6] Suru V , Bitoleanu A, Linca Mihaita, Indirect Current Control of a Filtering and Regeneration System used in DC Substations for Urban Traction, Athens Journal of Technology & Engineering, Vol. 4, No. 1, March 2017, e-ISSN: 2241-8237 (listed in the National Library of Greece).

[7] P.Ghani A.A.Chiane H.M.Kojabadi, An adaptive hysteresis band current controller for inverter base DG with reactive power compensation, 1st Power Electronic & Drive Systems & Technologies Conference, 978-1-4244-5971-1/10/$26.00 ©2010 IEEE.

[8] CV Suru, M Dobriceanu, GE Subtirelu, Direct current control by constant frequency hysteresis controller in active filtering systems, 2017 5th International Symposium on Electrical and Electronics Engineering (ISEEE), Galati, Romania, 20-22 Oct. 2017, **Electronic ISBN:** 978-1-5386-2059-5, **USB ISBN:** 978-1-5386-2058-8.

[9] Hansruedi Buhler, Réglage par mode de glissement, Presses Polytechniques Romandes, 1986, ISBN 2-88074-108-4.

[10] Mazari B, Mekri F, Fuzzy Hysteresis Control and Parameter Optimization of a Shunt Active Power Filter, JOURNAL OF INFORMATION SCIENCE AND ENGINEERING 21, 1139-1156 (2005), University's Power Engineering Conference UPEC 2001, 12-14 September 2001, Swansea, U.K.

[11] Constantin Vlad Suru, Mihaita Linca, Alexandra Preda, Eugen Subtirelu, Design and Analysis of the Compensating Capacitor Charging Algorithm for Active Filtering Systems, Conference: 17th IEEE International Power Electronics and Motion Control Conference (PEMC) SEP 25-28, 2016, Book Series: IPEMC Pages: 889-896 Published: 2016, ISBN:978-1-5090-1798-0.

[12] Constantin Vlad SURU, Cristina Alexandra PATRASCU, Mihaita LINCA, The Synchronous Fundamental dq Frame Theory Application for the Active Filtering, Annals of the University of Craiova, Electrical Engineering series, No. 38, ISSN: 1842-4805, 2014, pp. 92-97 (indexata Index Copernicus).

[13] Suru V., Popescu Mihaela, Pătraşcu Alexandra, Using dSPACE in the Shunt Static Compensators Control, Annals of The University of Craiova, No 37, 2013, ISSN 1842-4805, pp 94-99.

[14] CV Suru, M Linca, E Subtirelu, DSP Control Implementation Particularities for an Active DC Traction Substation Experimental Model, Conference: 10th International Symposium on Advanced Topics in Electrical Engineering (ATEE) Location: Bucharest, ROMANIA Date: MAR 23-25, 2017, Sponsor(s): Univ Politechnica Bucharest, Fac Elect Engn; IEEE, 2017 10TH INTERNATIONAL SYMPOSIUM ON ADVANCED TOPICS IN ELECTRICAL ENGINEERING (ATEE) Book Series: International Symposium on Advanced Topics in Electrical Engineering Pages: 607-612 Published: 2017, ISBN:978-1-5090-5160-1.

[15] CV Suru, M Linca, GE Subtirelu, Implementation of indirect current control for a active DC traction substation experimental model, Published in: International Conference on Optimization of Electrical and Electronic Equipment (OPTIM) & 2017 Intl Aegean Conference on Electrical Machines and Power Electronics (ACEMP), 2017, 25-27 May 2017, Electronic ISBN: 978-1-5090-4489-4 USB ISBN: 978-1-5090-4488-7, Page(s):630 – 635.